PERGAMON

International Journal of Multiphase Flow 27 (2001) 393–413

International Journal of Multiphase Flow

www.elsevier.com/locate/ijmulflow

Effect of particle motion on the wall's thermal structure and on heat transfer

G. Hetsroni*, M. Gurevich, R. Rozenblit, L.P. Yarin, G. Ziskind [1]

Department of Mechanical Engineering, Technion — Israel Institute of Technology, Haifa, Israel

Received 18 July 1999; received in revised form 1 April 2000

Abstract

Experiments with spherical particles sliding and rolling in cocurrent and counter-current directions over a heated wall have been conducted to study the mechanism of heat transfer in a turbulent flow carrying coarse particles. The detailed distribution of the local temperature and heat transfer coefficient in the vicinity of moving coarse particles was obtained. Results of experiments show the effect of the particle motion and rotation on the temperature distribution of the heated wall and on the heat transfer in the turbulent boundary layer.

Keywords: Heat transfer; Particle-laden flow; Thermal structure; Coarse particle

1. Introduction

Heat transfer in particle-laden flows is of a significant practical importance in modern engineering and technology. The interaction between particles and near-wall turbulent structure provides a research topic of both theoretical and practical interest. For example, particle motion and rotation determine, to a great extent, the heat transfer for fluidized beds and dilute particle-laden flows. That was the reason for performing numerous theoretical and experimental investigations of this problem, generalized in a number of

* Corresponding author. Tel.: +972-4-829-2058; fax: +972-4-832-4533.

E-mail address: hetsroni@tx.technion.ac.il (G. Hetsroni).

[1] Present address: Department of Mechanical Engineering, Ben-Gurion University of the Negev, P.O. Box 653, Beer-Sheva 84105, Israel.

0301-9322/01/$ - see front matter
PII: S0301-9322(00)00031-8

monographs and surveys (Soo, 1990; Boothroyd, 1971; Crowe, 1998; Hetsroni, 1984). At present, there are extensive data dealing with the effect of solid admixture on heat transfer in turbulent boundary layer (Han et al., 1991; Murray, 1994). They are related, mainly, to mean characteristics of the process and do not regard the mechanism of complicated phenomena due to near-wall particle/flow interaction. The latter occurs under conditions of a particle sliding and rolling in a predominantly shear flow. On the other hand, a coarse particle introduces strong disturbances in the turbulent boundary layer and affects the structure of the near-wall flow.

The significant practical importance of the problem attracted attention of a number of researchers, who proposed various models describing the phenomenon. In particular, Subramanian et al. (1973) assumed that the enhancement of the heat transfer due to particle motion near the wall is caused by "film scraping" and "particle convection". The term "particle convection" means that, while leaving the near-wall region, the particles themselves take the heat away to the bulk flow. Particle convection plays a dominant role in the heat transfer in gas-particle flows with small-size particles. The significance of the film scraping begins to increase with the particle size increasing or in liquid-particle flows. The investigation conducted by Verma and Rao (1987) shows that the increase in heat transfer due to a sphere moving parallel to a flat plate is larger and lasts longer in a liquid medium than in a gaseous one. Hence, to obtain detailed data on the heat transfer enhancement by coarse particles, one should study the particle motion in liquid flow.

It is well-known that the near-wall region of the turbulent boundary layer possesses a rather complicated structure which results from a strong interaction of large-scale vortices with low-speed streaks existing in the viscous sublayer (Kline et al., 1967; Head and Bandyopadhyay, 1981; Gad-el-Hak and Bandyopadhyay, 1994; Falco, 1991). Particles in turbulent near-wall flows interact with coherent structures. This interaction leads to a drastic change of the flow field: the low-speed streaks break up, migrate from the wall, etc.

The experiments of Rashidi et al. (1990) and Kaftori et al. (1995) showed that the near-wall particle/turbulence interaction manifests itself in the change of a level of turbulent fluctuations and bursting period. The particles of smaller sizes are generally accumulated along the low-speed streaks as shown in a direct numerical simulation by Pedinotti et al. (1993). They found that the degree of sorting depended on the particle dimensionless time constant, defined as $t_p = \rho_p d_p^2 u_*^2 / 18 \nu^2 \rho_f$ (here d_p and ρ_p are the particle diameter and density, u_* is the friction velocity, ν is the kinematic viscosity of the fluid, and ρ_f is the fluid density). The maximum sorting is obtained for values of t_p of about 3. This result is in partial agreement with the experimental observations (Hetsroni and Rozenblit 1994; Kaftori et al., 1995; Niño and Garcia, 1996). Hetsroni and Rozenblit (1994) showed that the particles near a wall change the level of temperature fluctuations at the wall and the value of the heat transfer coefficient.

Detailed data on the effect of stationary coarse particles located on the wall, on the heat transfer in turbulent boundary layer, have been obtained by Hetsroni et al. (1995). It was shown that in the vicinity of a coarse particle, the heat transfer coefficient increases 1.5–3 times as compared to the undisturbed flow. It was hypothesized that the increase in the heat transfer rate was due to the relative velocity between the particle and the fluid near the wall, which caused inrush of the cold fluid into the wall region. Data on the influence of the stationary

coarse particles for different types of particle arrangements (single particles of various sizes, a string of particles, etc.) on the local heat transfer coefficient were generalized by Hetsroni et al. (1997).

Particle rolling due to its interaction with solid surface and velocity gradient in the near-wall flow may also lead to heat transfer enhancement in the turbulent boundary layer. The latter is connected with turbulence modulation associated with coarse particles and their influence on low-speed streaks, bursting process, etc. The influence of particle rotation in unbounded flows was studied by Best (1998).

Although there are numerous investigations on particle-laden flows, there is no sufficient explanation of particle influence on the heat transfer. In particular, there is no data on the role of particle sliding and rolling over the wall on the heat transfer in the turbulent boundary layer.

The present study aims to fill this gap. For this purpose, we built an experimental set-up which makes it possible to establish particle motion with prescribed velocity and to study the influence of particle sliding and rolling on the heat transfer by means of an infrared technique and image processing. As a result, we obtain detailed information on the temperature field on the wall for a particle moving both in cocurrent and counter-current directions under various flow conditions where the ratio of particle diameter to the sublayer thickness is different.

When a coarse particle moves over the wall in a particle-laden flow, its motion is characterized by both sliding and rolling, depending on different parameters of the flow and the surface. Pure sliding and pure rolling are two limiting cases of a particle motion. Therefore, in the present study, we investigate these two cases, assuming that all other situations stay between them.

2. Experimental

The experimental facility is shown schematically in Fig. 1. The experiments were performed in a flume, see Fig. 2. The flume has already been described by Hetsroni and Rozenblit (1994), and only the main hydraulic parameters are presented here. The flow system is a stainless steel open channel 4.3 m long, 0.32 m wide and 0.1 m deep and water of constant temperature was recirculated in it. The flow is provided by a centrifugal pump and the flow rate is measured by a flowmeter. Care was taken to eliminate vibration, wave formation at the inlet and reflections from the outlet.

The test section (a part of the channel which is heated) was located at a distance of 2.5 m from the channel entrance. The constantan heater (on an isolated frame) was made of a foil 0.32 m long, 0.2 m wide and 50 μm thick. The window of the frame was 0.3 m long and 0.15 m wide. The foil was attached to the window by means of a contact adhesive, and was coated on the air side by a black paint of about 20 μm thickness. Uniform heat flux was achieved by applying DC power to the foil.

The surface temperature of the constantan foil is affected by the turbulent flow over it and is measured by an IR Imaging Radiometer. The radiometer was placed under the heater plate at a distance of about 0.5 m. Preliminary calculations have shown that the difference between the temperatures of the two sides of the foil is less than 0.1°C.

The minimum detectable temperature difference of the radiometer is 0.1°C at 30°C. Through calibration, the radiometer is very accurate in a narrow temperature range giving typical noise equivalent temperature difference (NETD) only, which is less than 0.2°C (with image average less than 0.05°C). A typical horizontal resolution is 1.8 mrad or 256 pixels/line.

A detailed analysis of the time-response of the heat-foil infrared technique has been done by Hetsroni et al. (1996). It was shown that the characteristic time of this method is much smaller than the characteristic time of the physical processes associated with the coherent structures and particle motion in the investigated range of the Reynolds numbers.

The experimental runs were conducted in our test facility as described above. The accuracy of the IR Radiometer (manufacturer's data) equals ±2%. The heat flux (DC power) was determined with the accuracy of 0.5%. Accordingly, the errors in measurements of the wall temperature and heat transfer coefficient did not exceed ±2% and 12%, respectively. The water depth and flow velocity were determined with accuracy of ±0.5% and 2%, respectively. The water temperature was measured by means of a precision mercury thermometer with accuracy of ±0.05°C. The errors in the Reynolds number did not exceed 2.6%.

A fully developed flow was established in the region beyond 2.5 m downstream from the entrance to the flume, which was confirmed by measuring the velocity distribution. The studies of thermal field of the heater plate were carried out at two values of Reynolds number, $Re_h =$

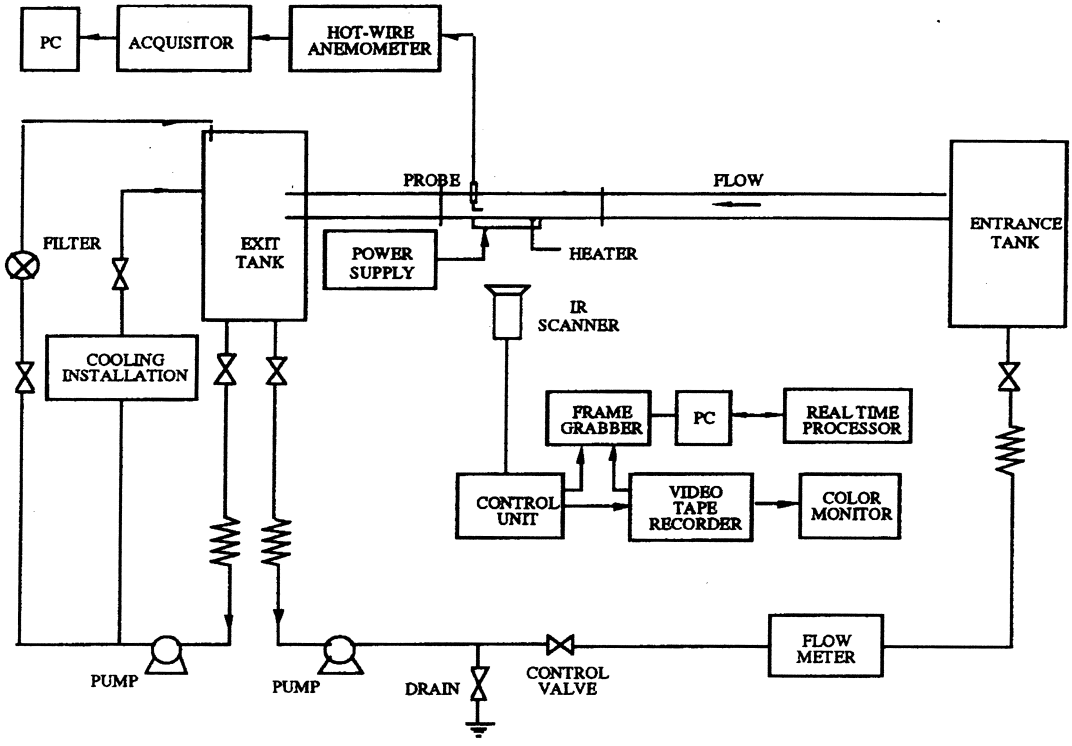

Fig. 1. Schematic description of the experimental set-up.

4300 and 6150. The temperature distribution on the wall can be considered as a trace of the flow structure near the wall, i.e. the structures in the turbulent boundary layer are the ones that cause the temperature distribution on the wall, including the thermal streaks.

A single spherical particle was placed on the heated foil, as shown in Fig. 2. By means of a thin steel wire, the particle was both slightly pushed against the wall and connected to a carriage which, in turn, was mounted on a screw. The screw was connected through a chain transmission to a special electric motor with controlled speed of rotation in the two directions.

During the investigation, the particle was dragged with a prescribed velocity along the centerline of the channel either in a cocurrent or counter-current direction, and its velocity was independent of the flow velocity. Also, in order to study the influence of particle rolling, we either fixed it on the wire or let it rotate freely.

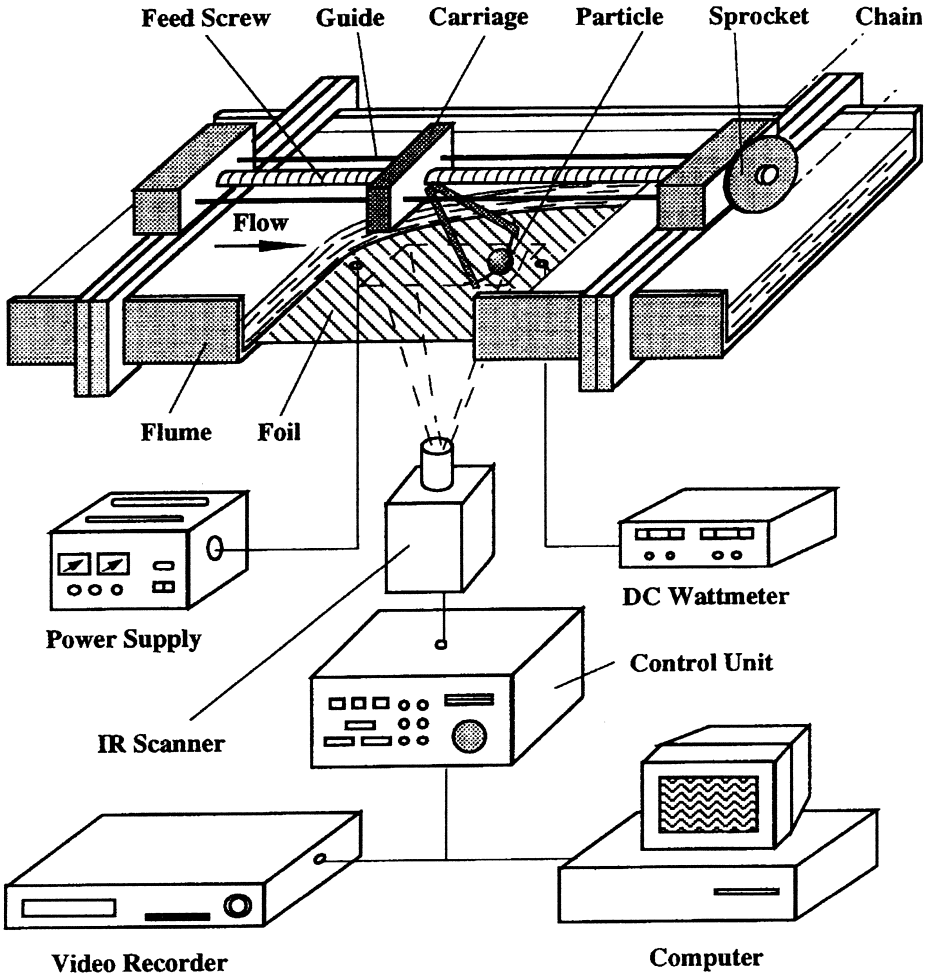

Fig. 2. Test section of the flume with a particle moving over the foil.

Table 1
General flow characteristics

Flow depth, h (cm)	Mean flow velocity, U_m (cm s^{-1})	Reynolds number, Re_h	Friction velocity, u^* (cm s^{-1})	Viscous sublayer thickness, δ_v (cm)	Mean wall temperature, T_w (°C)
6.7	7.70	6150	0.43	0.098	23–28 $\pm$ 0.2
6.7	5.88	4300	0.35	0.129	23–28 $\pm$ 0.2

The flow conditions and particles characteristics are presented in Tables 1 and Table 2. Here the signs "plus" and "minus" correspond to cocurrent and counter-current particle motion, respectively.

The range of the Reynolds numbers $Re_h = U_m h/\nu = 4000$–6000, based on the mean flow velocity U_m and flow depth h, at which the measurements were carried out, corresponds to a developed turbulent flow in a flume. The particle Reynolds number $Re_p = u_r d_p/\nu$, based on the particle diameter d_p and on the relative particle velocity u_r, defined as the difference between the velocity of the center of the particle u_p and the flow velocity as if taken at the same point u_c, was within the range $110 < Re_p < 1500$. Note that since in our experiments, particle velocity was always smaller than the local flow velocity, we conveniently consider Re_p as positive, with $u_r = u_c - u_p$. On the other hand, the Reynolds number of particle rotation $Re_\omega = \omega d^2/\nu$, based on the angular velocity of particle rotation ω can be both positive or negative and varied within the range $-700 < Re_\omega < 700$. Under these conditions, the flow in the boundary layer over the particle is distinctly separated. The size of the particles ($d_p = 5 - 20$ mm) used in the present experiments considerably exceeds the thickness of the viscous sublayer δ ($d_p/\delta = 2 - 8.5$). This fact allows one to estimate the contribution of disturbances introduced in the sublayer, as well as in the logarithmic region of the flow, on the temperature field on the wall.

Table 2
Particle motion characteristics. ($Re_h = 4300$, $u^* = 0.35$ cm s^{-1}, $\nu = 0.009$ cm^2 s^{-1}, $h = 6.7$ cm)

Particle material	Particle diameter, d_p (cm)	Particle velocity, u_p (cm s^{-1})	Angular velocity, ω (s^{-1})	Flow velocity at $h = d_p/2$, u_c (cm s^{-1})	Particle Reynolds number, Re_p	Angular Reynolds number, Re_ω	d_p/h	d_p/δ_v
Plastic	0.5	−1.6–1.6	−6.4–6.4	3.73	118–296	−178–178	0.075	3.88
Glass	0.78	−1.6–1.6	−4.1–4.1	4.13	219–497	−277–277	0.116	6.05
Glass	1.0	−1.6–1.6	−3.2–3.2	4.35	305–661	−356–356	0.150	7.75
Plastic	2.0	−1.6–1.6	−1.6–1.6	4.95	745–1455	−711–711	0.30	15.5

3. Flow characteristics

In order to establish the general flow characteristics and obtain a basis for comparison, we first performed a number of runs in pure water without any disturbances. The measurements of velocity were performed at the centerline of the flume, i.e. at $z = 0$ (z denotes the spanwise direction). Velocity measurements were done by means of a hot film anemometer. The standard 90° conical probe was connected to a traversing mechanism having a spatial resolution of 10 μm. The anemometer signal was transmitted through an acquisitor to a PC. The hot-film probe was calibrated in the water flume, and after the calibration, the sensor was positioned in the boundary layer and the data were recorded. The uncertainty in a measurement of the streamwise velocity is estimated to be about 2–4%; the highest value corresponds to the lowest velocity. The measurements showed that a fully developed flow was established in the region beyond 2.5 m downstream from the inlet to the flume.

The profiles of the mean velocity at $300 < Re_\theta < 600$, where Re_θ is the momentum thickness Reynolds number, are plotted in Fig. 3. The solid line in this graph corresponds to the logarithmic law $u^+ = 2.5y^+ + 5.0$ ($u^+ = u/u^*$, u and u^* are the local and friction velocities, respectively). The profiles of velocity were fitted to this line by adjusting u^*, so that the experimental values of u^+ and y^+ agreed with the "law of the wall". The present distribution of the friction velocity u^* is in agreement with the measurements by Rashidi et al. (1990) and

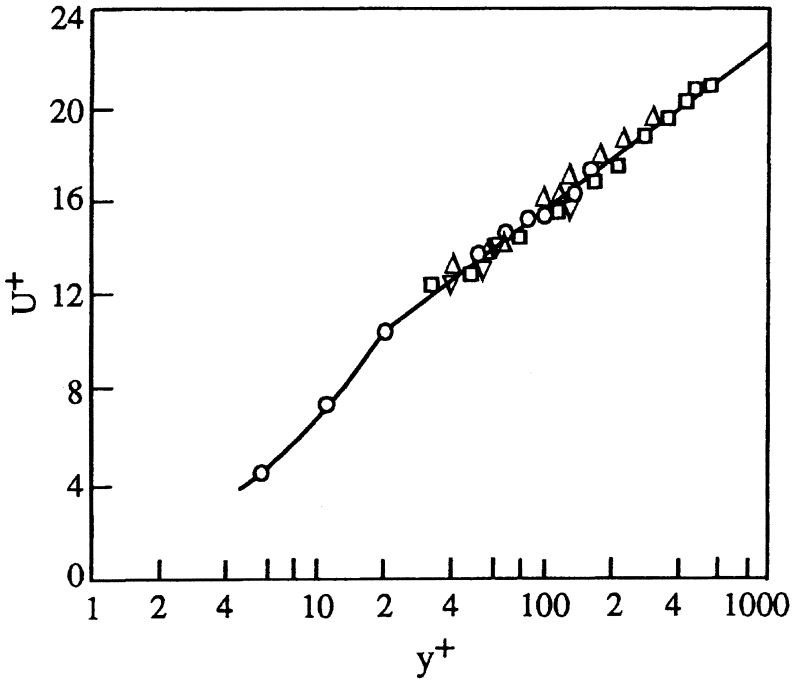

Fig. 3. Distribution of the mean velocity near the wall (channel flow) — the logarithmic law over a smooth wall: $u^+ = 2.5 \ln y^+ + 5$; ▽ — $Re_\theta = 300$, △ — $Re_\theta = 470$, □ — $Re_\theta = 600$; ○ — data by Antonia et al. (1992).

Kaftori et al. (1994), who used an identical flume. In Fig. 3, the data by Antonia et al. (1992) are also presented. These results agree fairly well with the data of the present experiments.

4. Image processing

The data from the IR radiometer were stored in a digital mode. For every set of flow and particle motion conditions, at least 20 runs were performed with a full record of the thermal field. The thermal fields for different flow conditions are depicted in Fig. 4.

In order to understand the influence of the particle on the heat transfer, one should separate it from a very complicated picture resulting from the coherent motions of the fluid in a near-wall turbulent flow. If it were possible to examine a thermal field with a particle and subtract from it the field on a smooth wall under the same flow conditions, the result would present the particle influence. However, because of the statistical character of the turbulent flow, such straightforward procedure is impossible.

In order to overcome this problem and obtain physically meaningful results, we use a procedure based on some threshold value of the temperature for which the influence of turbulent streaks is negligible. The threshold temperature is defined as the lowest instantaneous temperature over the flat wall without particles, as a result of turbulence/wall interaction.

For example, consider the thermal field in Fig. 5a. One can see that in the vicinity of the particle, and behind it, the structure is rather different from the structure far from the particle. It is obvious that the latter structure is the same as the one on a smooth wall. One can also see that in the vicinity of the particle, the temperature is, generally, lower than when far from it. Thus, for *every* thermal map, we use some threshold temperature value below which the influence of the streaks may be neglected. It should be stressed that the heat flux on the wall is the same both without and with the particle on it.

The thermal maps were then analyzed using the TherMonitor image-processing software. Color pictures were transformed into grayscale, see Fig. 5b. The software makes it possible to establish a certain temperature level and distinguish all the points where the temperature is lower than the threshold. These points form a cold spot, where the temperature is higher than the temperature of the fluid but lower than the average temperature of the wall.

We start from the lowest temperature recorded for this field (about 22°C for the example presented) and raise it gradually until some pixels appear far from the particle, and these are considered as caused by the streaks. Thus, the highest threshold value at which the faraway pixels do not appear provides us with the region with distinct particle influence — shown as blue spots in Fig. 5b.

The software makes it possible to determine the area of every spot and its minimal and mean temperature.

5. Analysis of the thermal structure

Thermal fields on the heated wall are shown in Fig. 4a–c for the different cases. Far from the particle, the temperature field has a streaky structure, characterized by alternating high and

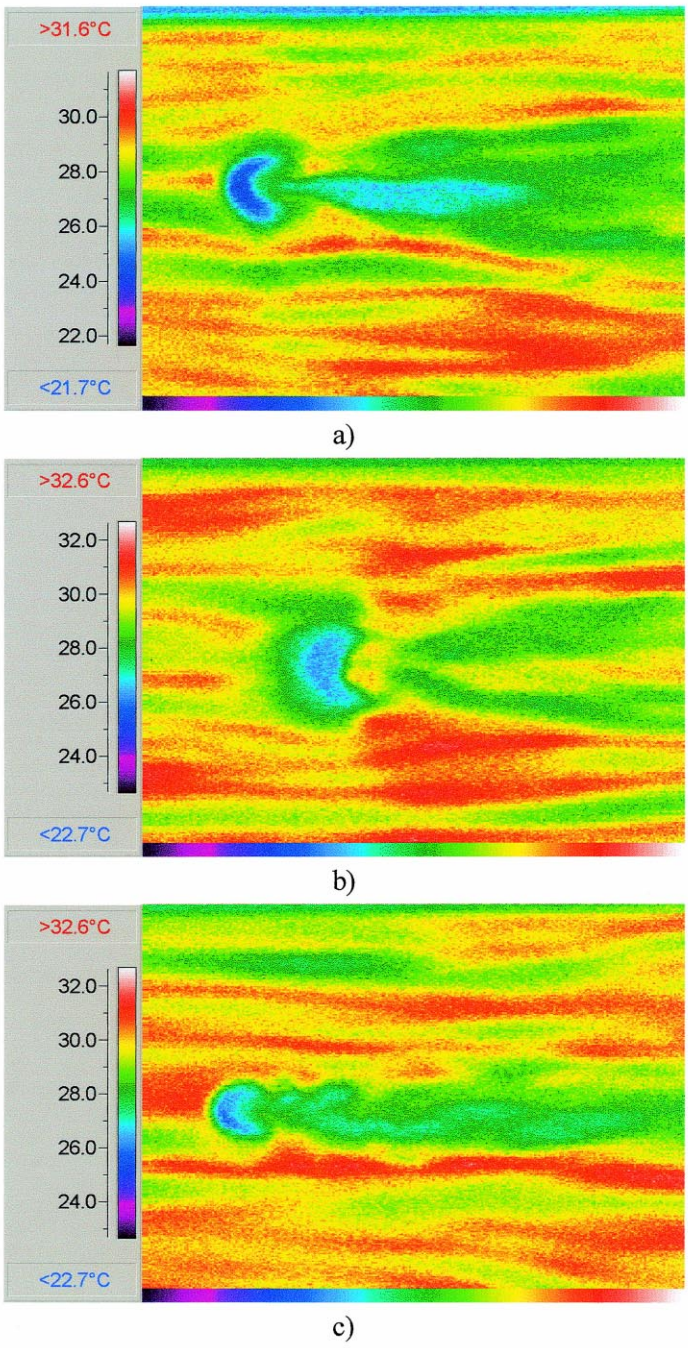

Fig. 4. Thermal field on the heated wall recorded by an IR radiometer (the flow is from left to right): (a) stationary particle; (b) cocurrent particle motion; and (c) counter-current particle motion.

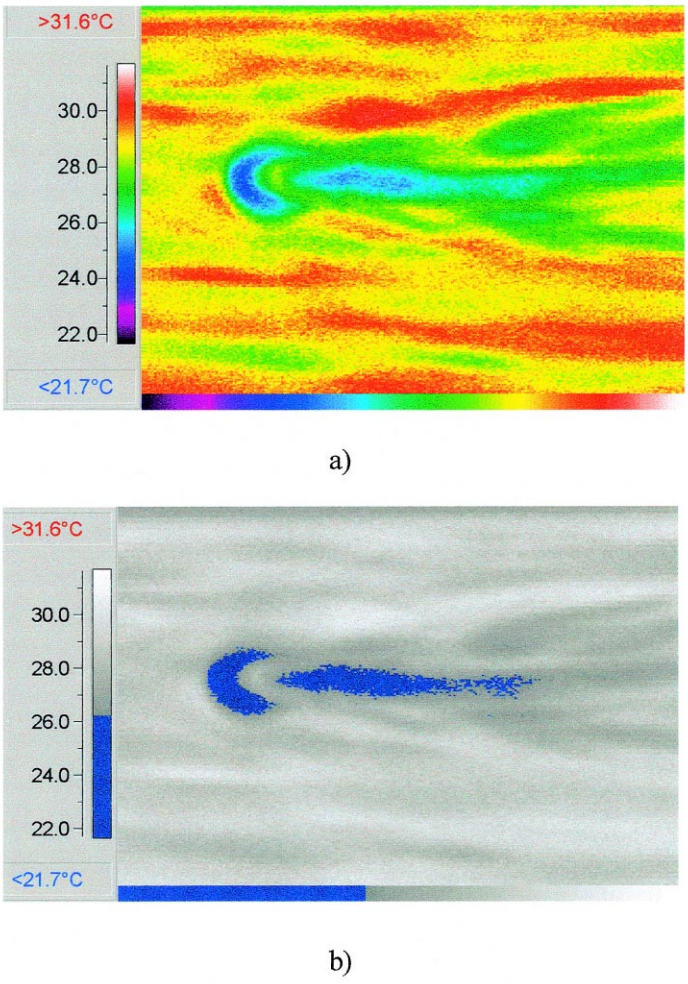

Fig. 5. Image processing of the temperature field in the vicinity of a coarse particle: (a) thermal field recorded by the IR radiometer; (b) the same thermal field with established threshold temperature.

low temperature regions stretched in the longitudinal direction. The dimensionless mean spanwise spacing between neighboring streaks equals approximately 100 wall units. Thus, the obtained temperature fields are in good agreement with the well-known results (Iritani et al., 1983; Simonich and Moffat 1982; Hetsroni and Rozenblit, 1994).

The disturbances introduced by a coarse particle lead to destruction of the velocity and temperature streaks and formation of low-temperature domains (spots) in front of and in the wake of the particle. The size and configuration of these domains depend (at fixed parameters of the channel flow) on the velocity and direction of the particle motion.

The low temperature spots in the vicinity of the stationary particle (Fig. 4a) have umbrella-like and ellipsoidal shapes, respectively, for the frontal and rear regions of the flow. The particle motion in the cocurrent direction leads to an expansion of the low temperature

domain, see Fig. 4b. This is a result of a decrease in the particle Reynolds number. Note that this expansion is not accompanied by a temperature change in front of the particle, whereas the temperature changes noticeably in the wake. More drastic change in the thermal spots occurs when the particle moves in a counter-current direction, i.e. its relative velocity is higher,

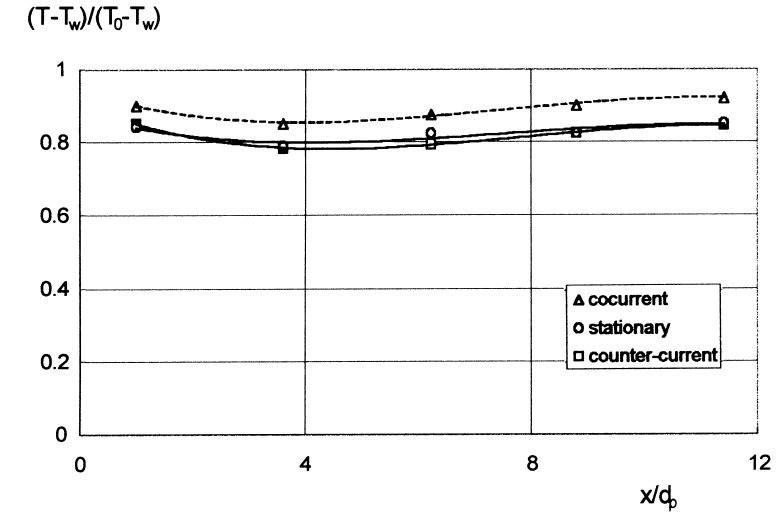

a)

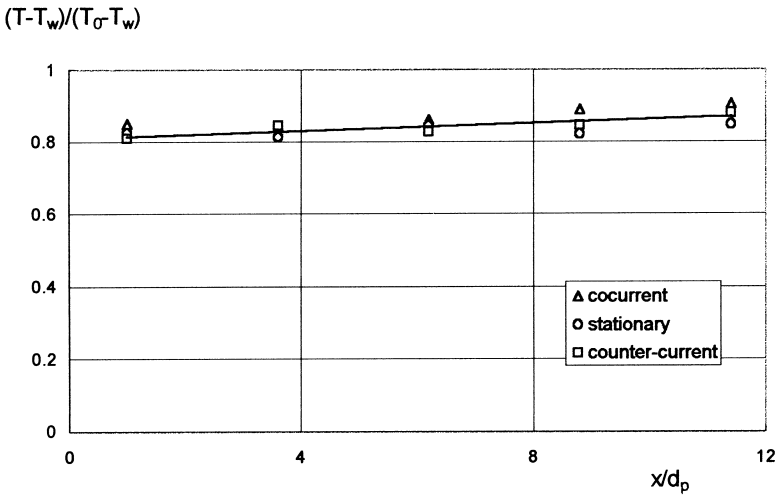

b)

Fig. 6. Temperature distribution along axis of the thermal spot behind the particle ($Re_h = 4300$): (a) sliding particle; and (b) rolling particle.

see Fig. 4c. This change expresses itself in shortening of the frontal spot and stretching of the one in the wake.

The shape of the low-temperature spots on the wall is due to the nature of the flow near a coarse spherical particle. The spherical shape causes the inrush of the cold fluid from the main stream towards the wall, in front of the particle, resulting in intensive cooling of the surface. Since the spherical particle has only one point of contact with the wall and streamlines embrace its surface, there is no circulation of the fluid near the point of contact in front of the particle. Hence, the heat transfer here is determined by the cold fluid inrush only.

The previous investigation (Hetsroni et al., 1997) has shown that the region behind an obstacle is of special interest for the heat transfer intensification. Therefore, we focus our attention on this region. The temperature distributions along the line up to $x/d_p = 12$ behind the particle ($x = 0$ at the particle center) are plotted in Fig. 6a, b both for sliding and rolling particles at $Re = 4300$. An intensive motion of the fluid behind the particle promotes smoothing of the temperature field in the longitudinal direction.

When the relative particle velocity is high enough, the temperature distribution in the longitudinal direction practically does not change within the range $1 < x/d_p < 12$. At low Re_p corresponding to a cocurrent motion, some increase in the dimensionless temperature $\overline{\Delta T} = (T - T_w)/(T_0 - T_w)$ is observed (T_w and T_0 are the average water temperature and the average temperature of the foil under undisturbed fluid, respectively). This increase is due to the decreasing rate of mixing between cold and hot masses of fluid in the near-wall region at low Re_p. Particle rolling (see Fig. 6b) enhances mass transfer in the vicinity of the particle and

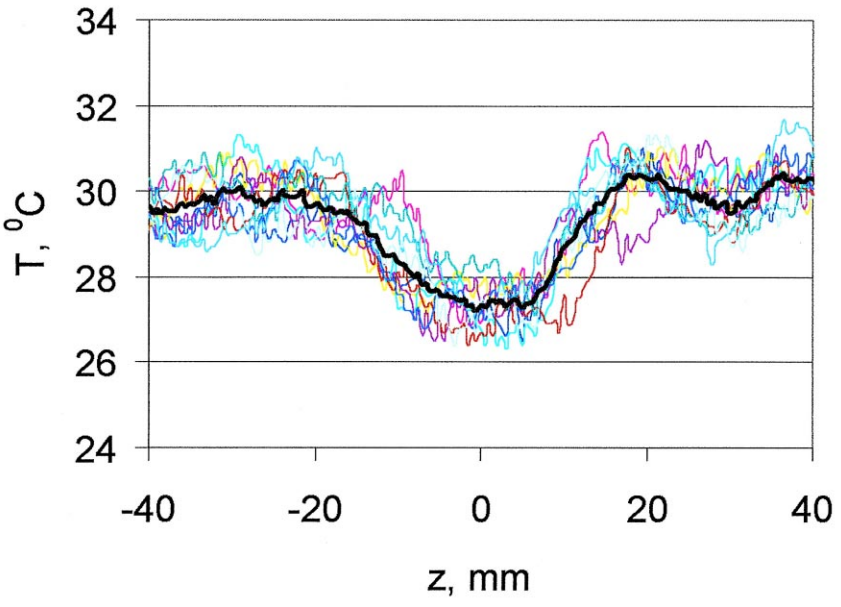

Fig. 7. Instantaneous (thin lines) and time-average temperature distribution in the thermal spot behind the particle (counter-current motion), $x/d_p = 5$.

causes damping of the effect of Re_p on the temperature field. One can see from Fig. 6a and b that there is no significant difference for the sliding and rolling particles.

The temperature distribution in the spanwise direction of a thermal spot is illustrated in Fig. 7. In this figure, instantaneous temperature profiles are shown together with the average one. The latter was found by averaging a number of instantaneous temperature profiles

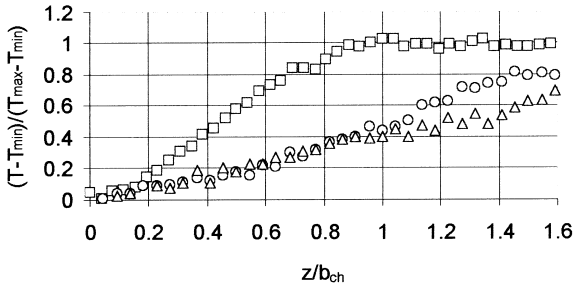

a)

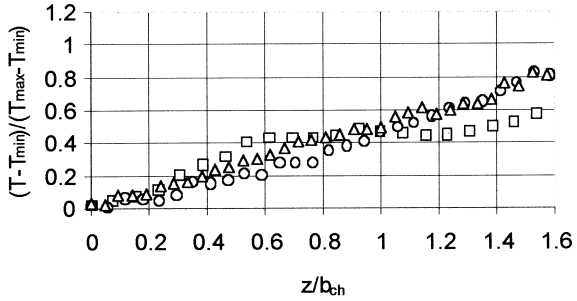

b)

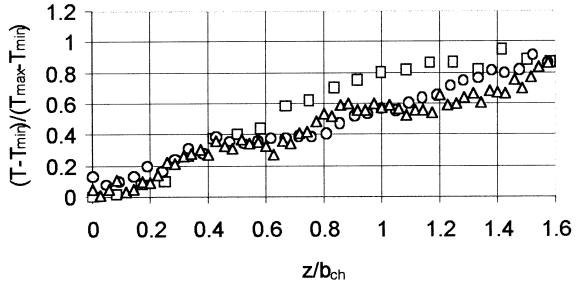

c)

Fig. 8. Dimensionless temperature distribution in different cross-sections of the thermal spot behind the particle (□ — $x/d_p = 2$, ○ — $x/d_p = 5$, △ — $x/d_p = 8$): (a) counter-current motion; (b) stationary particle; and (c) cocurrent motion.

recorded at different time instants. It is important to note that the heat flux remains constant. Hence, the time-averaged temperature distribution reflects (inversely) the map of the time-averaged local heat transfer coefficients.

In spite of significant fluctuations in the instantaneous temperature and some asymmetry relative to the particle centerline, the profiles of average temperature are symmetrical enough. This fact makes it possible to generalize the data on average temperature distribution in the form of dependencies of the dimensionless temperature versus transversal coordinate normalized to a width of the thermal spot. The dimensionless temperature was defined as $(T - T_{\min})/(T_{\max} - T_{\min})$, where T is the local temperature, $T_{\max}$ and $T_{\min}$ are the maximum and minimum temperature in the given cross-section. Taking into account that the temperature distribution in the non-disturbed domain is not uniform, we calculated $T_{\max}$ as an average of 50 points of this domain. The characteristic width b_{ch} was defined as a coordinate z at which $T = (T_{\max} + T_{\min})/2$ for every cross-section. The results of this generalization are shown in Fig. 8a–c. One can see that the experimental points corresponding to different cross-sections of the thermal spot group near one common curve $(T - T_{\min})/(T_{\max} - T_{\min}) = f(z/b_{\mathrm{ch}})$ for cocurrent motion. This trend also exists for stationary and counter-current cases, however, one can see that in the latter case, the results are more scattered.

Variation of the normalized width $2b_{\mathrm{ch}}/d_{\mathrm{p}}$ of the thermal spot with the distance x/d_{p} from the particle, for different particle velocities, is shown in Fig. 9. It can be seen that in all the

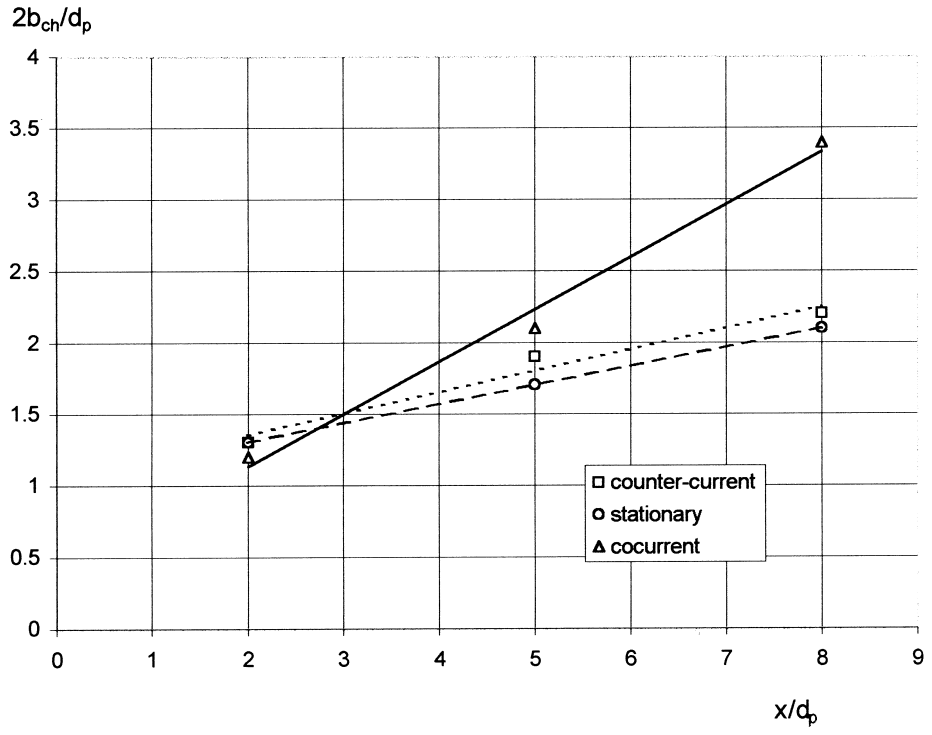

Fig. 9. Variation of the normalized characteristic width of the thermal spot behind the particle.

cases, $2b_{ch}/d_p$ increases practically linearly with x/d_p. The rate of the increase depends on the relative particle velocity. It is maximal at low u_r corresponding to a cocurrent motion. An increase in particle Reynolds number leads to a smaller rate of growth of the thermal spot.

If the particle is allowed to roll, its rotation also affects the width of the spot. Its influence is different for the co- and counter-current motion. Our experiments show that for the cocurrent motion, the spot behind a rolling particle is wider than that behind a sliding one. On the contrary, for the counter-current motion, the spot behind a rolling particle is narrower than that behind a sliding one. This fact is probably associated with change of the flow conditions which leads to a shift of the separation point on the particle surface.

6. Generalized results

The near-wall region of turbulent boundary layer presents a domain of an essentially non-uniform flow with linear velocity distribution within $0 < y^+ < 5$ (Schlichting, 1979) and feeble increase of velocity at $y^+ > 5$. A coarse particle larger than $y^+ = 5$ affects both regions of the flow: the sublayer and logarithmic part of the boundary layer. From the physical considerations, it is possible to expect that the disturbances introduced by particles in the sublayer and buffer zone play a dominant role in momentum and heat transfer.

On the other hand, considering the influence of a coarse particle on the flow field and heat transfer, we assume that the parameters of the particle itself, like its shape and dimensions, manifest themselves clearly when the particle is stationary. Therefore, we assume that the characteristics of the flow and the thermal fields around a stationary particle can serve as a common basis for generalization of the experimental data for moving particles. Naturally, for a moving particle, one should take into account the effect of its motion, presented by its velocity, in addition to the fluid velocity inside the sublayer.

In the previous investigation (Hetsroni et al., 1997), we performed a basic dimensional analysis of the flow and heat transfer in the vicinity of a coarse particle fixed on the wall in the turbulent boundary layer. The relevant dimensionless groups have been found. Therefore, we focus the present analysis on the additional parameters accounting for the particle motion.

From the physical considerations, for a particle submerged into shear flow, one can conclude that any flow field characteristic depends on the relative particle velocity and the shear. In accordance with this conclusion, it is possible to obtain one dimensionless group which is a ratio of the flow velocity difference across the particle $u_s = u_1 - u_2$ to its relative velocity defined, at the center of the particle as $u_r = u_c - u_p$, see Fig. 10a. This ratio is a so-called shear parameter (Legendre and Magnaudet, 1998). It is obvious that this shear parameter may be represented as a ratio of the two Reynolds numbers, namely, the shear Reynolds number and the particle Reynolds number Re_p (see, for example, Cherukat and McLaughlin, 1994).

This approach is valid for the case where the particle diameter is smaller than the thickness of the shear layer. When the particle is only partially submerged into the shear layer, see Fig. 10b, certain difficulty arises in the determination of the parameter on which the whole problem depends. As mentioned above, we assume that the dominant role in the transport processes is played by that part of the particle, which is submerged in the shear layer. The analysis presented below is based on this assumption.

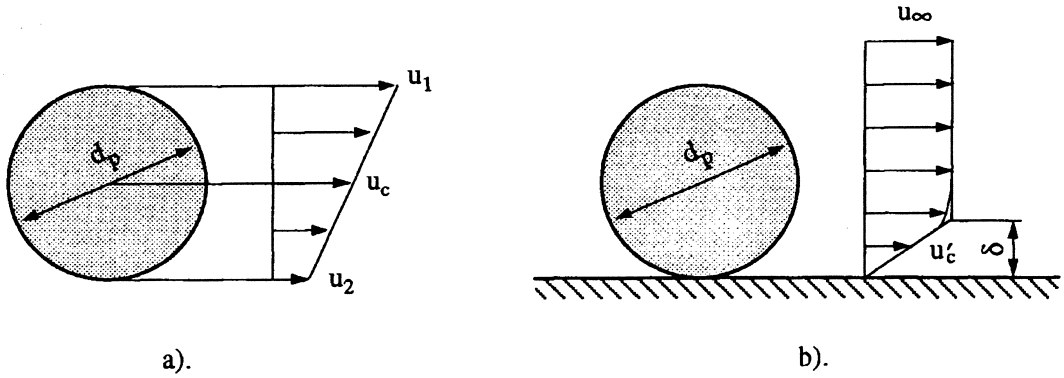

Fig. 10. Schematic description of the flow: (a) unbounded shear flow; and (b) near-wall flow.

Consideration based on the theory of similarity shows that in the present problem there are a number of parameters accounting for the specific properties of the particle, its velocity, and the shear layer characteristics. If we are interested in a certain parameter (e.g., an area of a thermal spot) of the flow or heat transfer related to a moving particle, we can consider the following list of four parameters

$$\Pi, \Pi_0, u_s, u_r \tag{1}$$

where Π_0 is the same parameter but for the stationary particle.

We note that u_r depends on the flow velocity as well as on the direction and magnitude of the particle velocity. We consider here a situation where the particle velocity does not exceed the flow velocity. This corresponds to the case of a particle-laden flow without external forces.

While considering these parameters, one can see that only two of them can have independent dimensions. Thus, according to the Buckingham π-theorem, two dimensionless groups can be formed, such that

$$F(\tilde{\Pi}, Sr) = 0 \tag{2}$$

where

$$\tilde{\Pi} = \frac{\Pi}{\Pi_0}, \quad Sr = \frac{u_s}{u_r} \tag{3}$$

Since the introduced parameter Sr is based on the flow velocity inside the shear region of the flow, we call it a "shear" criterion. It is a function of the flow and particle velocities, with its physical meaning representing the effect of particle motion in comparison to that produced by a stationary particle.

Solving Eq. (2) for $\tilde{\Pi}$, we obtain

$$\frac{\Pi}{\Pi_0} = \varphi\left(\frac{u_s}{u_r}\right) \tag{4}$$

where for a stationary particle $\varphi(0) = 1$, i.e. $\Pi = \Pi_0$. Thus, any parameter that depends on the particle motion can be expressed, related to the same parameter for an identical stationary particle, as a function of a single dimensionless parameter Sr. An exact form of Eq. (4) should be established experimentally.

The shear criterion Sr may be written as (Fig. 10)

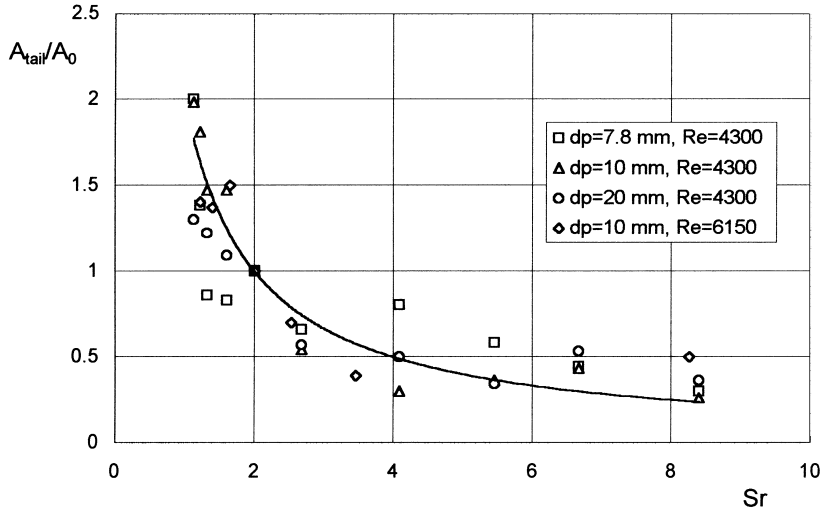

a)

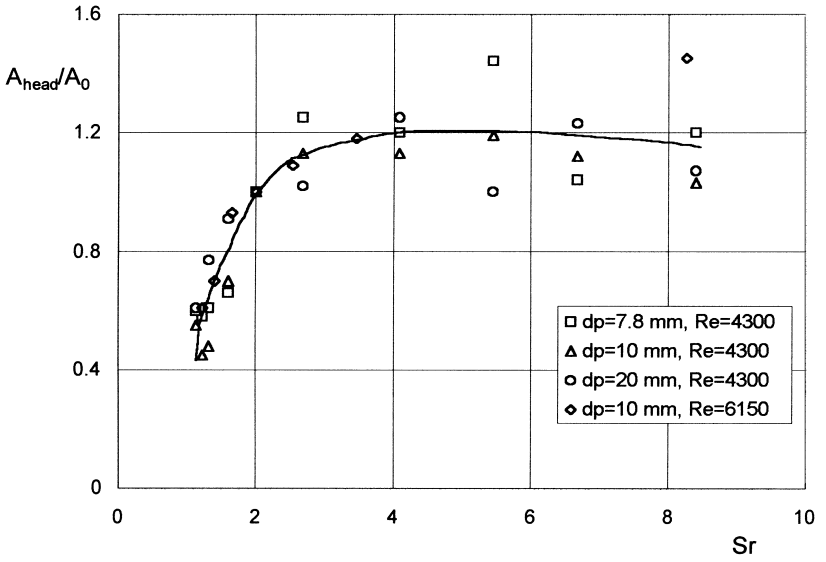

Fig. 11. Normalized area of the thermal spot as a function of the shear criterion: (a) the spot behind a particle; and (b) the spot in front of the particle.

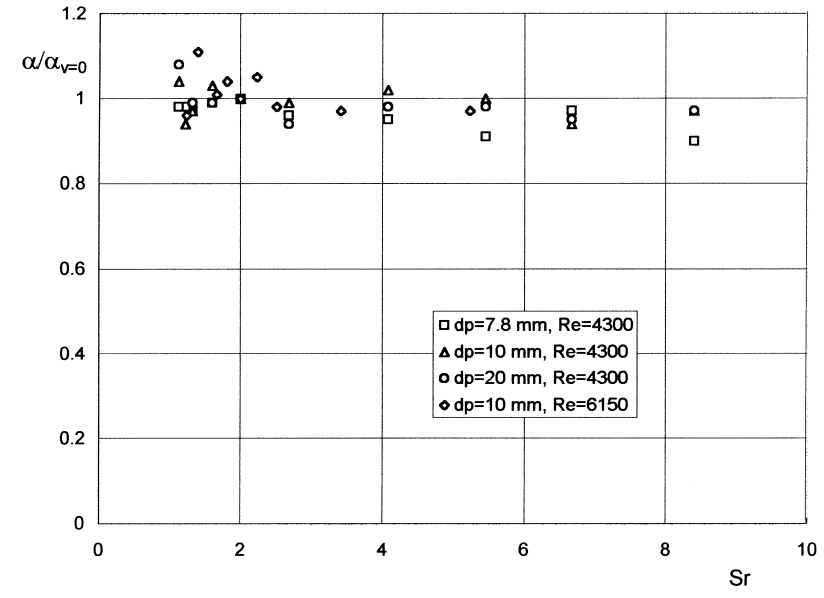

a)

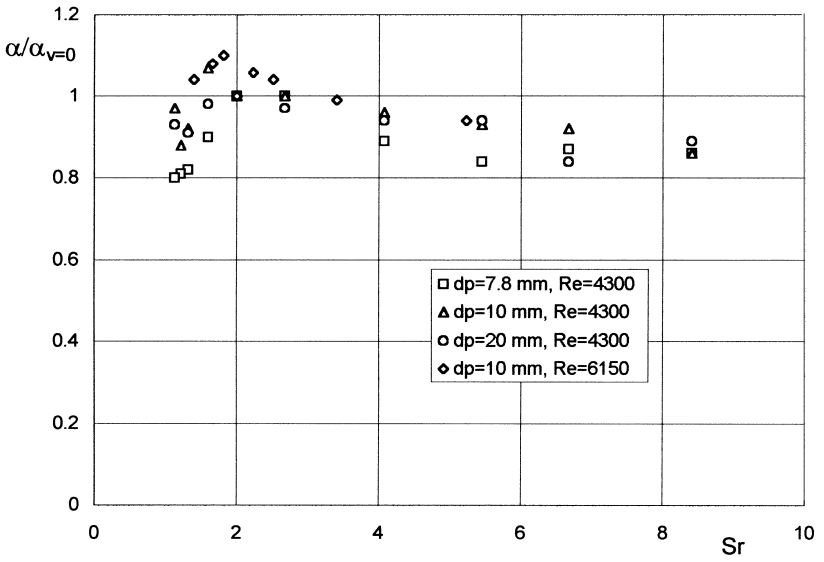

b)

Fig. 12. Normalized heat-transfer coefficient as a function of the shear criterion: (a) the spot behind a particle; and (b) the spot in front of the particle.

$$Sr = \frac{u_s}{u_r} = \frac{u_1}{u'_c - u_p} = \frac{2}{1 - u_p/u'_c} \tag{5}$$

where u'_c is the flow velocity at $y^+ = \delta/2$, and u_p is the particle velocity; δ is the characteristic thickness of the near-wall region where particle-caused disturbances interact with the streaky structure. The value of δ was chosen as the dimensionless height $y^+ = 12$, i.e. the point of intersection of linear and logarithmic profiles. Note that this value is also close to the critical roughness height (Schlichting, 1979). Since we use a linear approximation up to $y^+ = 12$, and taking into account that a particle in our case always touches the wall, the velocity difference across the layer becomes $u_1 = 2u'_c$.

We assume that the particle influence on the temperature field on the wall may be characterized (integrally) by the surface area of the thermal spots. The latter depends on a number of parameters accounting for the particle size, magnitude and direction of its velocity, velocity distribution in the near-wall flow, etc. In accordance with the similarity analysis presented above, we consider the ratio A/A_0 as a function of Sr only. It can be readily shown that the parameter Sr is some function of the ratio of the particle Reynolds number Re_p, based on the particle diameter and relative velocity, to the shear Reynolds number Re_γ, based on the particle diameter and the flow shear rate. The dependence $Sr(Re_p/Re_\gamma)$ is general for both the cases i.e., when the particle diameter is either larger or smaller than the thickness of the viscous sublayer.

The data on the average thermal spot areas are presented in Fig. 11a and b. One can see that the data corresponding to various conditions of external flow ($4300 < Re < 6150$) as well as particle velocity and size ($7.8 < d_p < 20$) group near two common curves $A/A_0 = \varphi(Sr)$, one for the frontal and the second for the rear spots, where A_0 is the area for a stationary particle, corresponding to $Sr = 2$. However, the nature of these dependencies is different. The area of the rear thermal spot decreases monotonically with Sr, whereas the dependence corresponding to the frontal spot has an extremum at $Sr = 4$.

The validity of the similarity analysis is supported by the experimental data not only for the thermal spot areas, but also for the heat transfer coefficients. Here, the parameter Sr allows a generalization of the data on the heat transfer intensity. The heat transfer coefficients were calculated from the constant heat flux and the time-averaged local temperature difference.

The data on the average heat transfer coefficient in the thermal spots corresponding to various conditions of the flow are presented in Fig. 12a and b. They show that the experimental points, corresponding to different particle sizes, magnitudes and direction of the flow velocity group near a common curve $\alpha/\alpha_0 = f(Sr)$, where α_0 corresponds to a stationary particle.

7. Conclusions

In the present work, an experimental study was carried out on the effect of the particle motion over a wall, on the temperature distribution and heat transfer from the wall. It was shown that the characteristics of the process depend on the direction of particle motion. The effects of particle rolling and sliding do not differ significantly.

The results of the present study confirm that the presence of coarse particles in the turbulent boundary layer leads to the destruction of the thermal streaks on the wall surface and formation of low-temperature spots in front of and in the wake of the particle. The front spot has an umbrella-like shape, whereas the rear one has the shape of a stretched ellipsoid. The temperature field inside the spots is practically uniform.

It is shown that there exists a universal shear criterion that allows generalization of both geometrical and thermal characteristics, including the areas of thermal spots and heat-transfer coefficient. This criterion is based on the characteristics of the viscous sublayer, and is suitable for the case when the particle diameter is much larger than the sublayer thickness.

Acknowledgements

This research was supported by the Technion VPR fund, Alexander Goldberg Memorial Research Fund, Miami Energy Research Fund, and the Fund for the Promotion of Research at the Technion. M. Gurevich and R. Rozenblit are partially supported by the Center for Absorption in Science, Ministry of Immigrant Absorption, State of Israel; L.P. Yarin is supported by the Israel Council for Higher Education.

References

Antonia, R.A., Teitel, M., Kim, J.L., Browne, W.B., 1992. Low Reynolds number effects in a fully developed turbulent flow. J. Fluid Mech. 236, 576–605.

Best, J., 1998. The influence of particle rotation on wake stability at particle Reynolds numbers $Re_p < 300$ — implications for turbulence modulation in two-phase flows. Int. J. Multiphase Flow 24, 963–972.

Boothroyd, R.G., 1971. Flowing Gas–Solid Suspensions. Chapman & Hall, London.

Cherukat, P., McLaughlin, J.B., 1994. The inertial lift on a rigid sphere in a linear shear flow field near a flat wall. J. Fluid Mech., 263, 1–18; 1995. Corrigendum, J. Fluid Mech., 285, 407.

Crowe, C., Sommerfield, M., Tsuji, Y., 1998. Multiphase Flows with Droplets and Particles. CRC Press, New York.

Falco, R.E., 1991. A coherent structure model of the turbulent boundary layer and its ability to predict Reynolds number dependence. In: Turbulent Flow Structure Near Walls. Cambridge University Press, Cambridge.

Gad-el-Hak, M., Bandyopadhyay, P., 1994. Reynolds number effect in wall-bounded turbulent flow. Applied Mechanics Review 47, 307–365.

Han, K.S., Sung, H.J., Chung, M.K., 1991. Analysis of heat transfer in a pipe carrying two-phase gas-particle suspension. Int. J. Heat Mass Transfer 34, 69–78.

Head, M.R., Bandyopadhyay, P., 1981. New aspects of turbulent-boundary structure. J. Fluid Mech. 107, 197–338.

Hetsroni, G., 1984. Handbook of Multiphase Systems. Hemisphere, New York.

Hetsroni, G., Rozenblit, R., 1994. Heat transfer to a liquid–solid mixture in a flume. Int. J. Multiphase flow 20, 671–689.

Hetsroni, G., Rozenblit, R., Lu, D.M., 1995. Heat transfer enhancement by a particle on a bottom of a flume. Int. J. Multiphase Flow 21, 963–984.

Hetsroni, G., Rozenblit, R., Yarin, L.P., 1996. A hot-foil infrared technique for studying the temperature field of a wall. Meas. Sci. Technol. 7, 1418–1427.

Hetsroni, G., Rozenblit, R., Yarin, L.P., 1997. The effect of coarse particles on the heat transfer in a turbulent boundary layer. Int. J. Heat Mass Transfer 40, 2201–2217.

Iritani, Y., Kasagi, N., Hirata, M., 1983. Heat transfer mechanism and associated turbulence structure in the near-wall region of a turbulent boundary layer. Turbulent Shear Flows IV, 223–234.

Kaftori, D., Hetsroni, G., Banerjee, S., 1994. Funnel shaped vortical structure in wall turbulence. Phys. Fluids 6, 3035–3050.

Kaftori, D., Hetsroni, G., Banerjee, S., 1995. Particle behavior in the turbulent boundary layer. 1. Motion, deposition, and entrainment. Phys. Fluids 7, 1095–1106.

Kline, S.J., Reynolds, W.C., Schraub, F.A., Rundstandler, P.W., 1967. The structure of turbulent boundary layer. J. Fluid Mech. 70, 741–773.

Legendre, D., Magnaudet, J., 1998. The lift force on a spherical bubble in a viscous linear shear flow. J. Fluid Mech. 368, 81–126.

Murray, D.B., 1994. Local enhancement of heat transfer in a particulate cross flow. Int. J. Multiphase Flow 20, 493–513.

Niño, Y., Garcia, M.H., 1996. Experiments on particle–turbulence interactions in the near-wall region of an open channel flow: implications for sediment transport. J. Fluid Mech. 326, 285–319.

Pedinotti, S., Mariotti, G., Banerjee, S., 1992. Direct numerical simulation of particle behaviour in the wall region of turbulent flows in horizontal channels. Int. J. Multiphase Flow 18, 927–941.

Rashidi, M., Hetsroni, G., Banerjee, S., 1990. Particle–turbulence interaction in a boundary layer. Int. J. Multiphase Flow 16, 935–949.

Schlichting, H., 1979. Boundary-Layer Theory. McGraw-Hill, New York.

Simonich, J.C., Moffat, R.S., 1982. New technique for mapping heat transfer coefficient contours. Rev. Sci. Instru. 53, 678–683.

Soo, S.L., 1990. Multiphase Fluid Dynamics. Science, Beijing.

Subramanian, N.S., Rao, D.P., Gopich, T., 1973. Effect on heat transfer due to a particle in motion through thermal boundary layer over a flat plate. Inc. Eng. Chem. Fundam. 12, 479–482.

Verma, A.K., Rao, D.P., 1988. Enhancement in mass transfer due to motion of a particle in experimental study. AIChE Journal 34, 1157–1163.